ELIoT

Enhance Lighting for the Internet of Things

DELIVERABLE: D4.4

Public Summary WP4

Contract number:	825651
Project acronym:	ELIoT
Project title:	Enhance Lighting for the Internet of Things
Project duration:	1 January 2019 – 30 June 2022
Coordinator:	Volker Jungnickel, Fraunhofer Heinrich Hertz Institute, Berlin ,Germany

Deliverable Number:	4.4
Type:	Report
Dissemination level	Public
Date submitted:	29.10.2021

Authors:	J.P. Linnartz, C.R.B Corrêa, T.E.B. Cunha, E. Tangdiongga, T. Koonen, X. Deng, M. Wendt, A.A. Abbo, P.J. Stobbelaar, P. Polak, M. Müller, D. Behnke, M. Martínez, S.Vicent, T. Metin, M. Emmelmann, S.M. Kouhini, K.L. Bober, C. Kottke and V. Jungnickel
Partners contributed	TU/e, SIG, WEID, MXL, KPN, FHG

ELIoT: Enhancing LiFi for a Next Generation Internet of Things

J.P. Linnartz[1,2], C.R.B Corrêa[1], T.E.B. Cunha[1], E. Tangdiongga[1], T. Koonen[1], X. Deng[1], M. Wendt[2], A.A. Abbo[2], P.J. Stobbelaar[2], P. Polak[2], M. Müller[3], D. Behnke[3], M. Martínez[4], S.Vicent[4], T. Metin[6], M. Emmelmann[6], S.M. Kouhini[7], K.L. Bober[7], C. Kottke[7] and V. Jungnickel[7]

[1]TU Eindhoven, [2]Signify, [3]Weidmüller Group, [4]MaxLinear, [5]KPN, [6]Fraunhofer FOKUS, [7]Fraunhofer HHI

***Abstract*—Communication for the Internet of Things (IoT) currently is predominantly narrowband and cannot always guarantee low latency and high reliability. Future IoT applications such as flexible manufacturing, augmented reality and self-driving vehicles rely on sophisticated real-time processing in the cloud to which mobile IoT devices are connected. High-capacity links that meet the requirements of the upcoming 6G systems cannot easily be provided by the current radio-based communication infrastructure. Light communication, which is also denoted as LiFi, offers huge amounts of spectrum, extra security and low-latency transmission free of interference even in dense reuse settings. We present the current state-of-the-art of LiFi systems and introduce new features needed for future IoT applications. We discuss results from a distributed multiple-input multiple-output topology with a fronthaul using plastic optical fiber. We evaluate seamless mobility between the light access points and also handovers to 5G, besides low power transmission and integrated positioning. Future LiFi development, implementation and efforts towards standardization are addressed in the EU ELIoT project which is presented here.**

Keywords— Future IoT, LiFi, Optical Wireless Communication, Light Communication, IEEE 802.11bb, ITU-T G.vlc

I. INTRODUCTION

The amount of wireless data traffic and the number of devices continues to grow at an exponential rate. This puts high pressure on the radio spectrum. Over the past decades, we have seen waves of innovation to enhance the bit rates (bit/s) and the density (bit/s/m^2) that can be provided by wireless radio networks, but the wireless technology needed to support this also becomes increasingly complex. For instance, massive multiple-input and multiple-output (MIMO) and beam-steering in 5G push the radio technology frontiers but may run into limits of complexity and power consumption also for signal processing and for conversion between analog and digital domains.

Reaching limits with RF motivates the industry into exploring new directions including optical wireless communications, which is also denoted as LiFi [1]. For light waves, walls, ceiling and floor are natural boundaries between the wireless cells that allow very dense reuse of a vast amount of optical spectrum. Light sources such as light emitting diodes (LEDs) can offer gigabits per second transmission with simple emitters and receivers, with the potential for very low cost.

The concept of communication via light is older than via radio. However, when local area networking (LAN) went wireless in the 1990's, the demand for achieving coverage across multiple rooms was larger than the desire to very densely reuse the radio spectrum, as at that time, not many devices were using it. That favoured radio solutions. Meanwhile, since the 1990s, Wi-Fi and cellular technologies became ubiquitous. The majority of the increased capacity is due to steadily reduced cell sizes as the need to serve many more users in dense areas grew. Extrapolating these trends explains the increasing interest in LiFi, which can cover small "personal" cells with very high data rates. Moreover, such a dedicated beam experiences and causes little interference from other users, thus can guarantee undisturbed, low latency traffic to its destined user.

Particularly, the Internet of Things (IoT) can be seen as a driving force behind further densification. The IoT is often characterized by a vast multitude of many devices that each generate only limited traffic, but collectively cause a substantial increase in traffic. However, as Figure 1 also illustrates, we foresee numerous future IoT applications that demand higher rates, lower latency, and increased link reliability. Examples are in factories with Industry 4.0 machines, industrial devices or smart glasses [2, 3]. LiFi is a promising approach to address these future needs, possibly combining the wider through-the-wall coverage of RF networks with high-density very small cell high quality of service (QoS) LiFi, as seamless handovers and a common security approach appear to be feasible, as work in this paper demonstrates.

The first LiFi systems are now deployed commercially, and further innovation and new features are needed to exploit its full potential in an increasing number of use cases and applications. This paper highlights how these challenges are addressed in the EU H2020 project ELIoT (Enhance Lighting for the Internet of Things). As this is an overview paper, extending our EuCNC paper [4] we refer the reader to multiple publicly available project papers for more details. In particular, the main contributions reported are:

- Providing and testing interworking with other systems such as the radio and wired infrastructure, in particular with 3GPP and 5G.
- Allowing mobility to other LiFi access points via MIMO link adaptation (horizontal mobility) and to other technologies, in particular with Wi-Fi and with 5G (vertical mobility) while protecting against outages from light beam blockage.
- Proposals for introducing MIMO and experimental performance verification by related G.hn home networking standards.

- Developing cost-effective and easy-to-install in-building backbone infrastructure networks, for instance plastic optical fiber (POF).
- Demonstrating end-to-end security concepts and comparing 5G and IEEE 802.1x approaches to security.

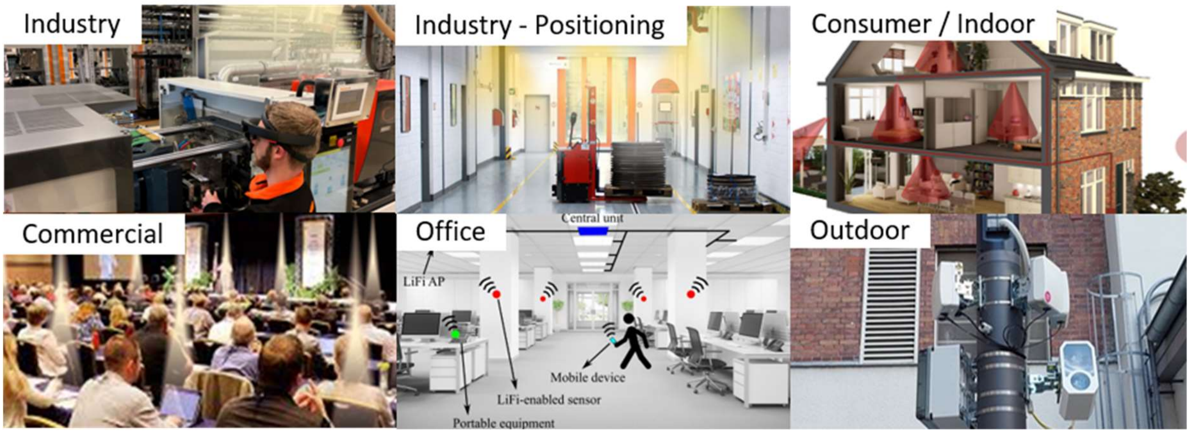

Figure 1: Some IoT use cases targeted by the ELIoT project.

II. LiFi Concept

There are many interesting applications for LiFi in different environments, such as office, industrial, in-home or outdoor [5]. Each of these poses different requirements, so a rigid single-use system concept may not be appropriate. However, cost and scalability considerations dictate that solutions for the various use cases can be served flexibly by functional components, exploiting commonalities and reusability of hardware and software. In fact, network integration of LiFi as a layer 2 LAN, equivalent to a classical Ethernet connection, is needed and provides good versatility by supporting various protocols such as the internet protocol (IP) or industrial automation protocols, see Figure 2. A common physical layer (PHY) and medium access (MAC) convergence format is important for harmonization. It addresses the key commonality of use cases and solutions.

The most widely used LiFi PHY makes use of direct current (DC)-biased orthogonal frequency-division multiplexing (OFDM) with adaptive bit loading to allow scalability and exploit the full capacity of LiFi. Distributed MIMO (D-MIMO) is an attractive extension as it supports spatial multiplexing and diversity [6, 7]. In fact, for industrial grade QoS, MIMO appears key to avoid link outages if a line of sight (LoS) is blocked [8].

As further elaborated in Section V.B, D-MIMO using spatially separated optical front ends (OFEs) can avoid frequent handovers associated with the small optical cell size, thus ensure consistent QoS and reliability for high mobility and high user densities. The MIMO PHY preferably is based on subcarrier-wise channel estimation. It can be based on feedback of the channel state information but can also exploit generic low-pass properties of LEDs [9]. To support battery-constrained devices, a low power PHY can be very useful. Biased pulse amplitude modulation (PAM) at a low rate, below the LED 3 dB bandwidth, in particular even below 3 MHz, proved to be effective in the uplink or in a visible light communication (VLC) downlink. It can coexist with OFDM in higher parts of the modulation spectrum, as popular high-speed (ITU) LiFi standards use frequencies above, say 5 MHz, while in this paper we focus on OFDM systems at these higher frequencies.

To ensure QoS with guaranteed throughput and latency, the channel access mechanism is reservation-based, using spatial time division multiple access (spatial TDMA), similar to Space-Time Reservation Multiple Access [10] . Power saving through scheduled sleep periods yields longer battery life times.

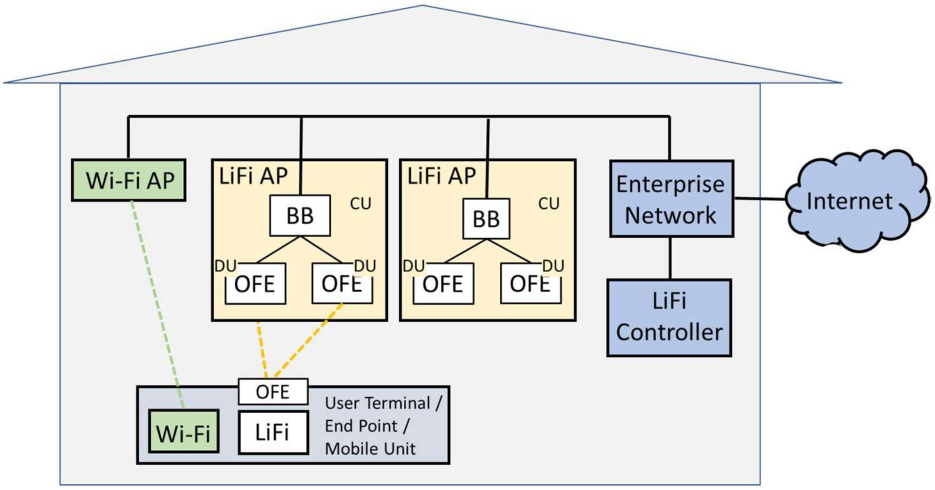

Figure 2: Indoor system architecture overview comprising LiFi and Wi-Fi: each LiFi access point (AP) has a LiFi central unit (CU) that performs the base band (BB) PHY and MAC layers and connects to multiple Distributed Units (DUs) which are optical front ends (OFEs) in the ceiling. The user terminal is also referred to as mobile unit (MU).

The backhaul connects the LiFi infrastructure to a fixed access network with a common interface to the higher layer services. This backhaul network may be realized over different media, such as ethernet, power line communications (PLC) and POF, each having its own capacity and latency characteristics. Whether or not a separate power infrastructure is needed for active optical front ends (OFEs) can also be a key design consideration if cost of the backbone is critical. A transparent ("analog, jitter free") fronthaul network allows versatile integration and upgradability. The identified main functional components of LiFi connectivity can be combined in order to build practical solutions for different use cases. Extended functionality for specific solutions can be realized through software modules in the CU (only). Further advanced functions can be link monitoring to facilitate vertical handovers, remote configuration based on standard protocols, as well as QoS management and service metering.

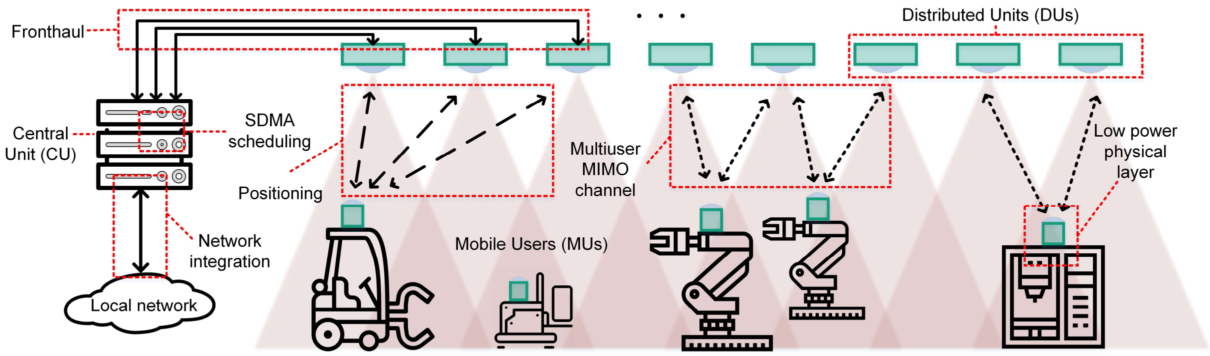

Figure 3: The distributed multiuser MIMO system architecture, depicting a CU connected with DUs via a fronthaul network. Mobile and stationary devices communicate via the LiFi infrastructure at the same time. Several key aspects are indicated.

Extending Figure 2, a LiFi system concept for an industrial scenario has been investigated in ELIoT [3, 11], and the concept may also be used in other situations. The concept is based on large-scale distributed MIMO to cope with the line of sight characteristics of light and the required QoS. A key aspect of our approach is to scale up the number of OFEs that are controlled by a single AP to cover larger areas. This AP can execute the PHY and MAC processing in a synchronous manner for all OFEs. As a result, moving users stay connected as the AP dynamically selects the appropriate set of OFEs. This enables virtually seamless connectivity without the need for handover protocol procedures. Moreover, centralized signal processing for the distributed OFEs facilitates the use of synchronous MIMO schemes to increase link robustness and throughput further. Figure 3 applies this to an industrial context.

Depending on the context, such APs are in literature and in standardisation referred to as central units (CUs) and distributed ceiling nodes, possibly luminaires, that are equipped with OFEs are denoted as distributed units (DUs), see Figure 3. Each DU can reach terminals or end points like mobile units (MU) in a certain area with its light cone. The cones of neighbouring DUs can overlap to provide homogenous coverage with adequate spatial diversity opportunities. There are multiple ways to split functionality between the CU and DUs [12, 13], but for indoor LiFi, we see an attractive approach in creating the waveforms in the CU and feed these over a transparent linear channel without digitization. A transparent and synchronous fronthaul network connects all DUs with their common CU. In fact, DUs are understood as the optical antennas of the CU, which receive analogue waveforms ready for transmission to and from the mobile users (MUs). In the CU, the PHY defines the transmitted waveform, including error coding and modulation, and aids the MAC through measuring the channel. As we will elaborate in Section IV, because the CU controls all MIMO processing for its DUs and MUs in the whole coverage area, no exchange of PHY-layer information between multiple APs (CUs) is necessary. Mobility is adaptively supported by adapting the signals to DUs for each MU based on the channel state. This can be done in various ways, such as by approaches that are similar to antenna combining or selection in radio systems, or power loading based on a total power constraint or per-DU power constraint [14]. IEEE 802.15.13 already makes use of different PHYs for downlink and uplink transmissions which may be attractive for other standards, for instance in ITU G.9991 [15]. Both are chosen such that they support the different requirements for downlink and uplink in an optimal way. Because MUs may be battery powered, the uplink PHY should be more energy-efficient and able to operate at a low signal-to-noise ratio (SNR) [16].

To select and track the best DUs based on the MU's mobility, an IEEE 802.15.13 scheduler in the CU considers the latest channel state. Moreover, the modulation and coding scheme (MCS) is selected carefully to optimize the rate while frame losses and increased latencies through retransmission are avoided. To obtain the necessary information for this scheduling, the CU assesses the channel between all its DUs and the MUs periodically. Moreover, features such as multi-user access and conflict-free scheduling are supported [11, 16].

Accurate positioning is considered an enabling feature for wireless communication in factories, e.g. to locate automated guided vehicles. For integrated positioning, the high-speed OFDM PHY can perform sub-sample accurate timing measurements based on a conventional ranging (also denoted as timing advance) aided by additional phase estimation in the frequency domain. If this approach is combined with distributed MIMO, the MAC can triangulate the position of the terminal and reach centimetre precision [18]. A detailed description of our approach can be found in Section X.

III. SECURITY

LiFi is said to be inherently more secure than radio. Light can be easily kept inside a room and signal levels outside a main light beam are inadequate to eavesdrop on the signal. The inherent protection against a jamming attack on a large industrial installation or factory hall becomes increasingly important in Industry 4.0 settings with autonomous devices. Nonetheless, this view disregards many types of potential attacks. So, we rather phrase the property that light stays inside the room as adding an additional layer of security. However, this does not obviate the need for proper encryption, authentication, access control, key management and hardware device security. If LiFi is used in security critical settings, the "digital" security needs to be at least as good as is common practice for radio-based infrastructures. For instance, bringing a hacked LiFi device into a secured area should not compromise the complete LiFi network security. IT departments or operators prefer to rely on security mechanisms that are compatible with commonly used industry standards, such as WiFi-compatible or 5G-based approaches, respectively.

The operator-focussed approach taken in ELIoT sees LiFi as a new access technology for non3GPP access to 5G network systems. The secured connection for the non3GPP access to 5G is accomplished through the encapsulation and encryption of the transferred packets. A 3GPP technical specification [19] has introduced a new component called N3IWF which is responsible for the access and session operations between the user equipment (UE) and the core network (CN). It realizes IPSec tunnelling from the UE to the N3IWF to control the data security in both 5G control and user planes. Internet key exchange (IKE) and extensible authentication protocols authorization and key agreement (EAP-AKA) generate the key pairs for packet encryption and decryption. In this way, encapsulation and protection of LiFi communications complies with common security standards.

A second approach, which is appropriate for enterprise networks, provides compatibility with the IEEE 802.1X standard [20]. This approach makes any LiFi device operates in similar way to a Wi-Fi device. The IEEE 802.1X standard defines a port-based network access control and authentication protocol that prevents an unauthorized client device from connecting to a LAN through publicly accessible ports unless they are properly authenticated. As shown in the following Figure 4, IEEE 802.1X systems use a standard client/server architecture including the following three components:

- A **Supplicant,** which is a software module running on the terminal device to be authenticated and providing credentials to the authenticator using EAPOL frames [20]. The credentials are provisioned in advance by the network administrator, and could include a user name/password, shared key or a cryptographic certificate [21].
- An **Authenticator,** which is a software module running on the access point that controls the access of the terminal device to the network, and that relays the communications between the authenticating device (using EAPOL frames towards the AP) and the authentication server (using RADIUS protocol towards the AP) [22].
- An **Authentication Server,** which maintains the trust relationships between terminal devices and the access network that can receive and respond to requests for network access originating from a terminal device running the supplicant. The server can evaluate the access requests and inform the authenticator if the connection is to be allowed for the device requesting the access. The authentication server runs software supporting the RADIUS and EAP authentication protocols [23].

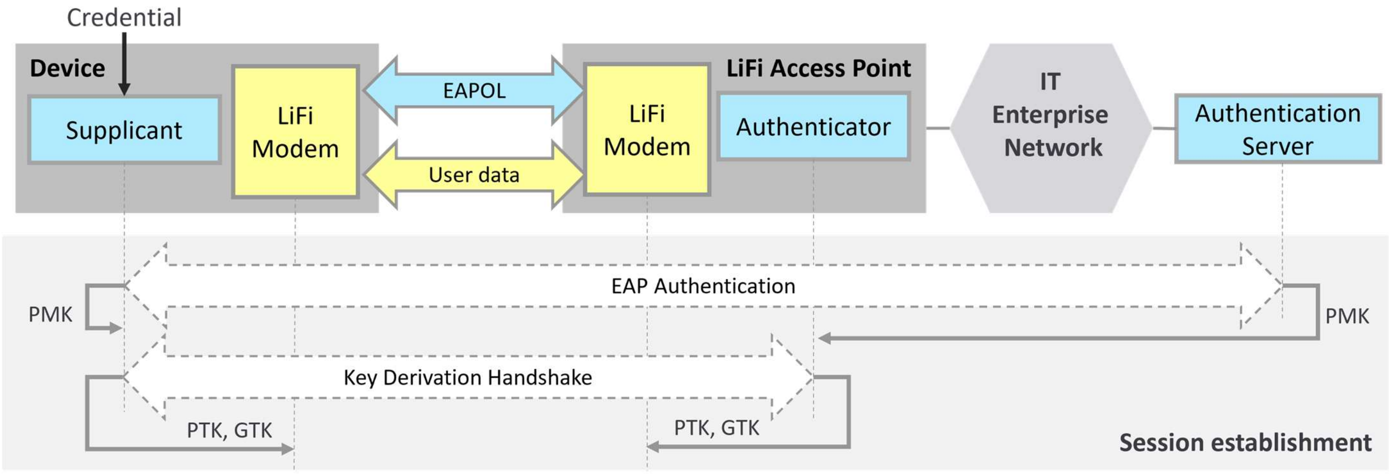

Figure 4: LiFi enterprise network deployment using IEEE 802.1x including the Supplicant, Authenticator and Authentication Server

The authentication exchange is carried out between the supplicant and the authentication server with the authenticator acting as a relay for the EAP messages. The EAP messages carrying the EAP method specific data are transported using EAPOL frames between the supplicant and the authenticator and RADIUS protocol between the authenticator and the authentication server, as shown in Figure 5 below.

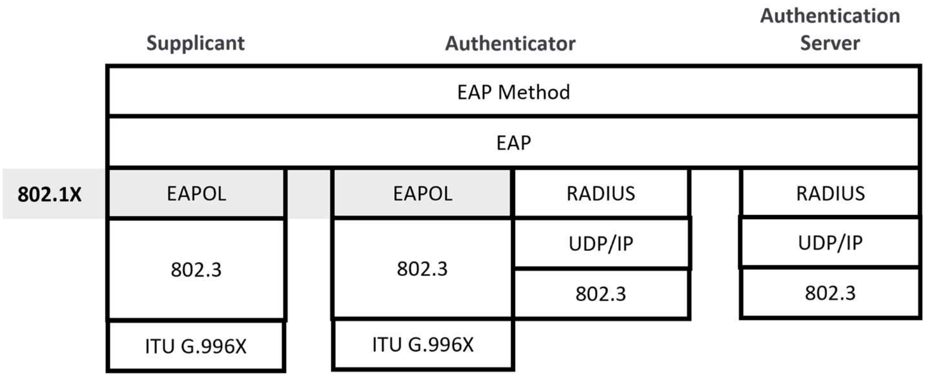

Figure 5: IEEE 802.1x port-based network access control protocol stack

The authenticator facilitating EAP between the supplicant and the authentication server ensures that no user data can be transferred through the access point before the device is granted with access and the secure session establishment involving device authentication and key derivation is finalized.

The following steps are performed for the secure session establishment:

- **Device and network authentication** through EAP method handshake between the supplicant and authentication server using pre-provisioned credentials, which results at both, the supplicant and the authentication server, in a common master key: pairwise master key (PMK).
- **Transfer of the PMK from the authentication server to the access point**
- **Key derivation handshake** (like 4-way handshake for Wi-Fi defined by [24] performed between the terminal device and the access point by using the master key, resulting in a set of specific transient keys: pairwise transient key (PTK) and group transient key (GTK) keys.

The PTK and GTK keys resulting from the key derivation handshake are used to derive session keys used to secure the data exchanged between the LiFi end point node in the client device and the LiFi access point over LiFi link. Once the session keys are derived, the device is granted with access to the network and a secure channel is established between the client device and the access point allowing user data to be securely exchanged. This concludes the session establishment exchange.

This approach provides not only full control over who is joining the enterprise network but also flexibility of supporting anyone of the standardised EAP authentication methods within the same infrastructure. A standardized set of commonly used protocols ensures that LiFi connectivity can easily be incorporated into any enterprise IT infrastructure.

IV. MOBILITY SUPPORT

Seamless large-area coverage involving multiple LiFi APs and the integration of radio-based networks like 5G and Wi-Fi are important topics in ELIoT. Different handover scenarios are investigated, each with different characteristics and requirements. Moreover, security and access aspects are addressed to allow the integration of LiFi into existing Wi-Fi and 5G radio networks [13]. Figure 6 shows the handovers studied, with the definition in Table 1 and a detailed description of various mobility scenarios below.

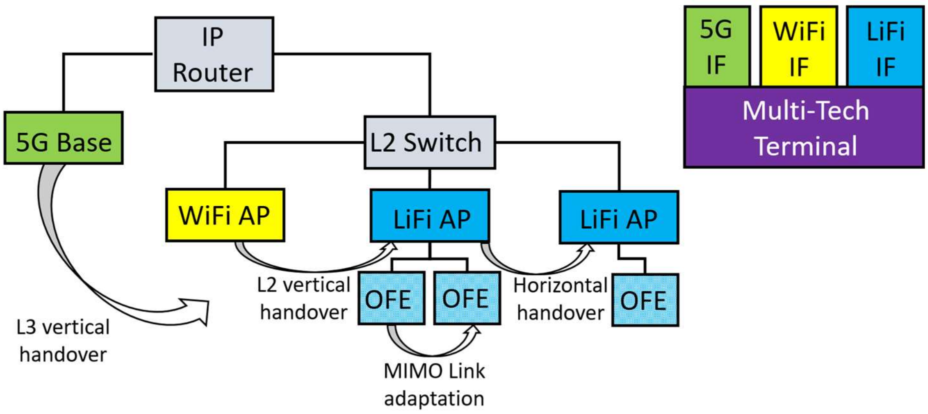

Figure 6: Handover scenarios between LiFi, Wi-Fi and 5G.

Table 1: Handover definitions between LiFi, Wi-Fi and 5G.

Term	Description / definition
MIMO link adaptation	A single AP optimizes the use of multiple OFEs to aid end point mobility. Association remains in the AP.
Horizontal handover	Transfers of association state between two APs of overlapping LiFi cells. This is independent of the interference coordination between the APs.
L2 vertical handover	Moves layer 2 connectivity between a Wi-Fi network and a LiFi network. The terminal's MAC address is preserved
L3 vertical handover	Moves IP-level connectivity of a terminal between different access technologies. The terminal's IP address might be preserved. Integration into 5G core network.

A. MIMO link adaptation within one LiFi AP

In this scenario, multiple OFEs provide LiFi access in a service area (e.g. a single room) via a common AP that adapts its MIMO PHY layer if mobility demands so. Through other OFEs, the LiFi AP keeps the connection to the terminal alive even if the line-of-sight towards one OFE is accidentally blocked. Moreover, if the terminal is moved or rotated, the connection is maintained. The LiFi AP and terminal may optimize link performance by taking advantage of the light traveling via different signal paths. This is realized by using the D-MIMO technology. If a terminal moves within the coverage area of the LiFi AP, the latter can adapt the connection to the terminal by changing the selection of active subset of OFEs for this terminal and by adapting the physical layer parameters (e.g. bit loading) for optimal link quality. The LiFi AP can trade-off between robustness and power consumption. For robustness, the AP may activate all its OFEs for a terminal. To reduce power consumption, the AP may activate only the best OFE.

B. Horizontal handover: Moving between APs with non-overlapping coverage areas

In this scenario, multiple areas are each served by a LiFi AP, whereby these areas are optically separated. This is typically the case for the situation of multiple (small) rooms in a building. No interference occurs between APs. If a terminal moves from one area to another, it typically enters an intermediate area (e.g. a corridor) without LiFi coverage and loses LiFi connectivity temporarily. As soon as the terminal re-enters an area with LiFi coverage, it re-connects (rapidly) to LiFi.

C. Horizontal handover: Moving between APs with overlapping coverage areas

In this scenario, a large area such as an open office space is served by multiple LiFi APs, each covering part of the total area. Now the coverage of APs intentionally overlaps to prevent dead zones. A terminal in an overlap area connects to one AP while interference has to be managed, e.g. by coordinating APs. Motion of terminals across service areas is similar to Wi-Fi: a terminal can initiate a handover. This

could be a “break before make” handover, whereby the LiFi link is lost, but most preferably a “make before break” handover is supported to keep breaks of the LiFi link short.
LiFi will have much smaller cells than Wi-Fi and more abrupt cell fringes. This demands a fast handover. A terminal therefore preferably anticipates a handover by pre-registering to a neighbouring AP and pre-establishing security keys via the currently active connection and the backhaul. The line-of-sight propagation characteristics of LiFi requires adequate handling of interference and hidden-terminal problems. A terminal typically sees the APs, but not any of the other terminals. An AP sees terminals but not the neighbouring APs. Hence, carrier-sense multiple access (CSMA) may not prevent APs (or terminals) from transmitting at the same time. LiFi preferably uses a coordinated medium access. This also strengthens the ability to guarantee QoS, by organizing the medium access so that the link is not hampered by interference.

D. L2 vertical handover: Moving in/out of LiFi area within a Wi-Fi area

In this scenario, a small area is served by LiFi (e.g. a single room), while a larger area is covered via Wi-Fi (e.g. in a hallway or in less intensively used rooms). For a terminal that moves in or out of the LiFi area, a vertical L2 handover between LiFi and Wi-Fi takes place. A terminal in the LiFi area can off-load the traffic from Wi-Fi and increases its QoS. A terminal that moves out of the LiFi area keeps a connection through Wi-Fi, as shown in Figure 6. Ideally, by aggregating two wireless techniques, their throughout is added. In the IEEE 802.11 standard, L2 handover is defined by fast BSS transition and fast session transfer. As LiFi is not yet tightly integrated into 802.11, alternatively, integration of both techniques can be realized via the IEEE. 1905.1 standard. In fact, 1905.1 existed already for some time but gained popularity as the Wi-Fi mesh technology reuses clauses from it.

E. L3 vertical handover in 5G context

Integration of LiFi into radio-based 5G connections requires a L3 vertical handover [13]. This enables a user to freely move between both 3GPP-trusted and untrusted access systems. The implementation in ELIoT of such a handover is shown in Figure 7.

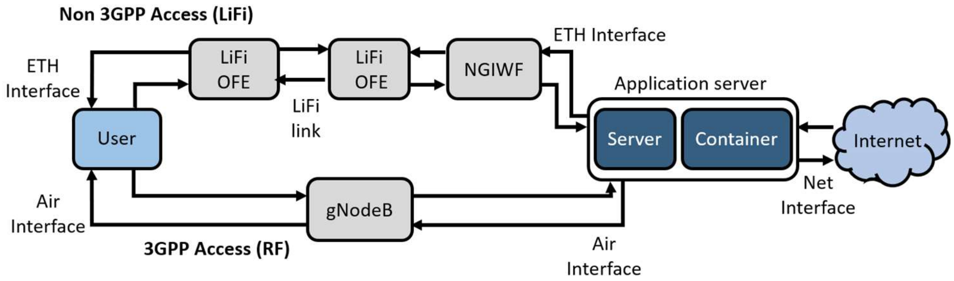

Figure 7: LiFi-5G integration, as experimentally implemented at test set up in ELIoT.

Building blocks on the left hand side of Figure 7 consist of a user terminal, e.g. a PC, which has parallel connections to the application server, by LiFi and by 5G new radio. The application server runs the 5G Core Network using software defined networking (SDN). The radio connection, i.e., the air interface, takes place on the 3GPP radio access network (RAN). As a mediator gNodeB is used, which represents the 5G RAN, and the core network, which is responsible to investigate the access operation. A second connection is created over an Ethernet interface ETH to the LiFi OFE, then through the actual LiFi wireless link to the infrastructure LiFi OFE, and finally via Ethernet to N3IWF coping with the integration of non-3GPP access technologies into the 5G packet core. In principle, the LiFi link is an untrusted connectivity. Thus, the integration of LiFi into a 5G system mandates to encapsulate and encrypt packets between the user terminal and the NGIWF before these are transferred over the air; regardless of any link encryption. This operation for non3GPP access has been implemented in ELIoT. The responsible 5G network function is named N3IWF and it makes sure that the IPSec tunnelling is established without flaws to match the security standards [13]. In the case of link failures, the integrated system is capable of switching between these two access networks with a very low latency and keeping user entities preserved.

V. INTER AND INTRA-CELL INTERFERENCE

To avoid that interference degrades performance inside cells or in overlap zones, one can divide the channel resources over the contending nodes. Multiple access is possible by time division (TDMA), modulation-frequency division (FDMA), code division (CDMA) or wavelength division (WDMA), provided that a flexible MAC protocol that can handle spatially conflicting demands. Radio systems, particularly those designed for unlicenced bands as used for IEEE 802.11, use carrier sense multiple access – collision avoidance (CSMA/CA), that is, a node “listens before it talks”. CSMA can flexibly handle random arrivals but may not guarantee QoS for ongoing sessions as it lacks the ability to reserve resources.

As indoor LiFi networks use line-of-sight propagation characteristics, CSMA faces hidden node problems. An upward looking MU or end point (EP) typically sees the downwards faced OFE of the APs, but not any of the other EPs. An AP sees terminals but not the neighbouring APs. Hence, CSMA may not prevent APs (or terminals) from transmitting at the same time. LiFi preferably uses a coordinated medium access within each cell. This also strengthens the ability to guarantee QoS, by organizing the medium access so that the link is not hampered by interference. In ELIoT, we focus on the ITU G.9991 standard that adopts TDMA for high QoS.

Continuous coverage implies that cells will overlap and potentially interfere with each other. So while moving between APs with overlapping coverage areas, not only a handover but also interference coordination of conflicting transmissions needs to be addressed spatially. A distinction from RF is that LiFi communicates via a directional LoS. This keeps the interference mostly localized to the overlap zone of the directly adjacent illuminated areas. In most cases leakage into remote cells is negligible, which is in contrast to rich multipath propagation in indoor radio systems. Our reference system contains ceiling-mounted LiFi APs while LiFi end points (EP) are spread in the area. Figure 8(a) depicts the coverage areas of AP1 and AP2 in solid grey and those of the EP1 and EP2 in dashed line, respectively. The red arrow in Figure 8(a) shows how AP1 interferes with AP2 transmitting to EP2 (white arrow down). AP2 may not detect transmissions from AP1. Figure 8(a) also shows that EP2 is a hidden node for EP1. LoS propagation limits the coverage to a specific cell, such as a specific machine in case of an industrial system. This makes it possible to densely reuse the optical spectrum, so that the full high data rates become available at each machine location in a factory hall.

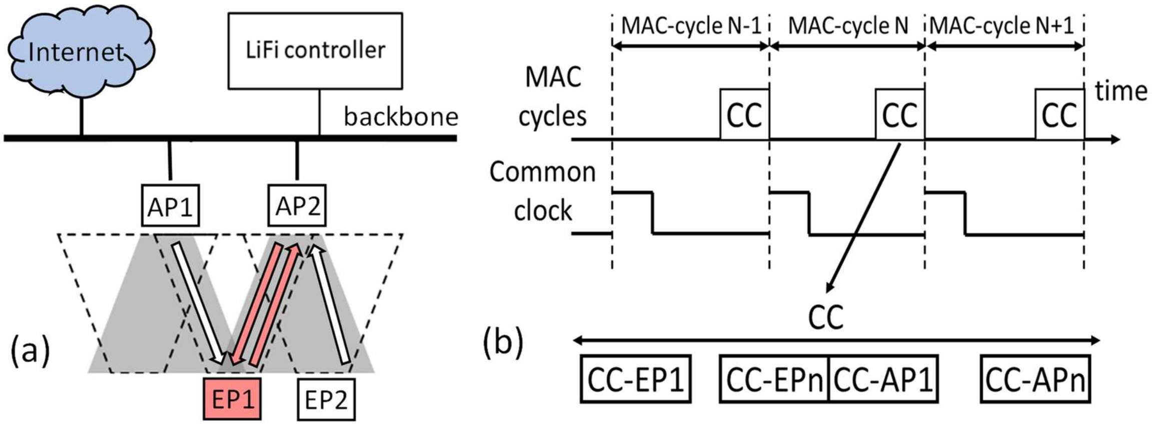

Figure 8: LiFi network consisting of fixed APs and mobile user terminals EPs (a) and MAC cycle alignment to common clock and CC (b).

LiFi is often promoted for its ability to provide contention-free QoS for ongoing sessions. In fact, TDMA allows coordinated scheduling. The network of APs determines the scheduling on the medium. Competition for access is resolved by coordinating the time-schedules within and among adjacent APs, where the latter becomes a spatial extension of TDMA. A common channel (CC) may be established in order to facilitate the exchange of information between domains and facilitate detection of the interference.

A. Spatial TDMA

The ITU-T G.9991 TDMA protocol can run as a specific firmware on ICs available for ITU-T G.9960/G.9961 [25]. ITU-T G.vlc separates the network into “domains”. A LiFi domain can contain multiple cells, thus multiple CAs, and is seen as a part of a larger LiFi network. The domain concept may also fit to IEEE. 802.11 standard, if a LiFi domain is regarded as a basic service set (BSS). All APs of one domain use a synchronized clock to ensure that TDMA frames are aligned across cells. Whether or not two neighbouring APs can simultaneously use the same slot depends on the interference levels seen by EPs in the overlap zone [17]. For OWC, we exploit the opportunity of connecting every domain via their AP to a backbone which exchanges inter-domain management messages via unique connections. Figure 8(b) shows this architecture. A dedicated LiFi controller (LC) handles and manages inter-domain contention, but does not act as a traffic router in the backbone. The LC observes instances of inter-domain interference and coordinates APs by setting constraints to their access schedules to avoid possible collisions, for instance using insights from [17]. The LC can be implemented as a central entity, but its functionality may also be distributed among the APs while the APs can nonetheless converge to a common, mutually coordinated scheduling. A common clock is shared among the domains to coordinate the MAC-cycles in multiple domains. Figure 8(b) shows how APs are synchronized. This can be realized by running the precision time protocol (PTP) according to IEEE 1588 over the backbone. APs and EP terminals advertise their presence over a CC to detect potential inter-domain interference. Every AP tracks the activity of neighbouring nodes and reports interference events (collisions) to the LC, to allow it to set scheduling constraints for adjacent APs to resolve any conflicts. We illustrate this for the scenario in Figure 8. In domain 1, EP1 receives advertisements of AP2 belonging to domain 2. AP1 flags this as an interference risk to the LC. In response, the LC constraints AP1 by only allowing transmission to EP1 in a limited set of timeslots. It also constraints AP2 by prohibiting this set of slots in any communication with its own EPs. The algorithm to set time-division constraints is left as an opportunity for proprietary innovation, as it does not need to be fixed in ITU-T G.9991. A certification authority may be needed to ensure interoperability of LCs, APs, and EPs from different vendors.

B. Handover-friendly and Interference-mitigating Cell Layout

In a basic spatially-extended LiFi network, every light point (e.g. a ceiling mounted luminaire) can become an OFE or even a full AP, so cell boundaries and handovers can occur in the middle between two such light points. In RF-based WLAN systems, co-located antennas can offer MIMO gains because of the multipath nature of indoor radio propagation. For a rich scattering RF environment, an antenna separation of just half a wavelength is known to be adequate for creating independent, thus MIMO-separable streams. In LiFi, this mechanism of random multipath wave cancellation is not seen, because the detector itself spans thousands of wavelengths. Hence, even for non-LoS LiFi with rich scattering of intensity-modulated LC, the detector averages out multipath randomness by non-coherently adding photon flows. To achieve MIMO gains OFE separation needs to be much larger than the wavelength of the light; it needs to be larger than c/f, where f is the modulation frequency (10 .. 100 MHz), thus many meters rather than micrometres. Co-location of optical MIMO OFEs in one device does not lead to independent channels, so a distributed architecture of MIMO OFEs is needed. Secondly, in optical propagation, the LoS is typically much stronger than the collective set of reflections, such that multipath does not yield a MIMO gain. Thirdly, and possibly most importantly, the LiFi channel statistics are dominated by blockage effects rather than by multipath wave cancellation.

If we consider these factors and the observation that the signal is most vulnerable in the middle between two light points where propagation distances are larger and where slant angles of arrival are more prone to blockage, we come to a cell layout, in which every cell is illuminated from its corners, as in Figure 9. Inside the area, mobility is supported by (MMO) link adaptation. Handover to an adjacent cell occurs right underneath each light point rather than halfway between APs. For the typical 60x60 cm ceiling tiles in offices, this calls for 90 degree corner sectors pointing into the cell with cell sizes of an integer multiple of the ceiling grid size, e.g. 1.8 or 2.4 m. The EP can of course rely on angular diversity, thus can be miniaturized.

The cell overlap zone now falls underneath a OFE and may be abrupt, thus the size of the overlap area will be mainly determined by the transition distance needed to execute a horizontal handover for typical EP speeds. For collimated sectors, thus when the sector boundary is sharply confined in azimuth rather than a gradually increasing lateral path loss, this handover line can be defined much more accurately for sector handover with in one OFE, then for a transition somewhere halfway between two spatially separated OFEs. Reducing the overlap area also reduces the need for interference protection at the MAC layer, thus reduces the need for inhibiting potentially conflicting emissions, thus the user capacity increases.

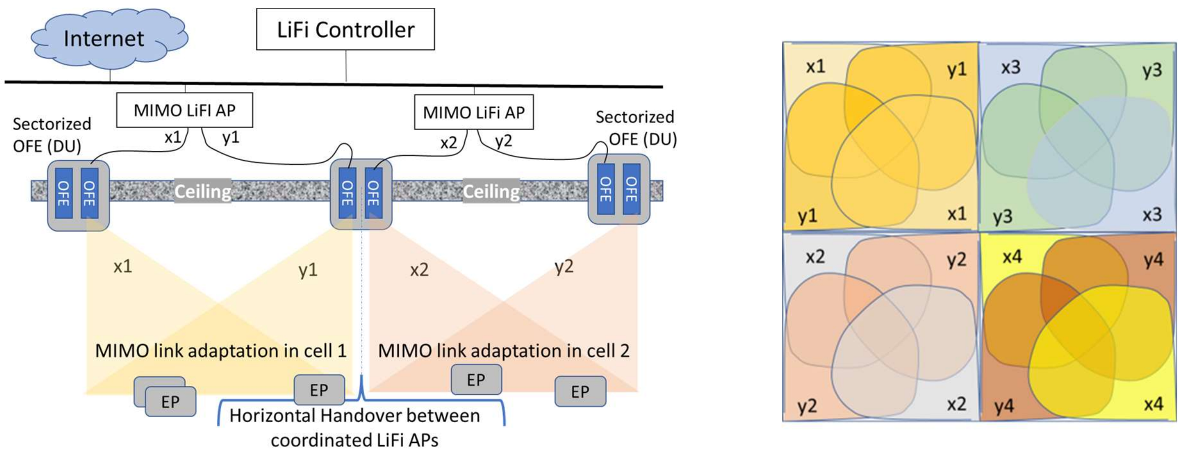

Figure 9: LiFi cell layout that places cell boundaries along collimated sectors. Horizontal handovers take place on a well-defined line, while soft MIMO link adaptation takes place in areas in between APs. Left: Cross section. Right: top view of MIMO channels x,y in cell 1, 2, .. 4.

VI. BROADBAND PHY FRONTHAUL

As argued before, LiFi needs D-MIMO to protect against link blockage. This section presents a fronthaul infrastructure and identifies how the architecture of the fronthaul can be (cost-) optimized by leveraging the MIMO capabilities to jointly address wireless crosstalk and possible crosstalk in the fronthaul infrastructure. To explain that, we initially model the concatenation of a fronthaul and a wireless channel from a MIMO perspective.

The end-to-end channel, including wireless and fronthaul, from N_T emitters to N_R receivers is described by a $N_R\ x\ N_T$ MIMO matrix $\boldsymbol{H}(f) = \boldsymbol{Z}(f)\boldsymbol{G}(f)$. That is the product of the crosstalk coefficients from the POF fronthaul link represented by $\boldsymbol{G}(f)$ and the coefficients of the spatial overlap in the wireless channel given by $\boldsymbol{Z}(f)$. That is, we found that the $\boldsymbol{Z}(f) = \boldsymbol{Z}_0$ is mostly constant over frequency and that the response of $\boldsymbol{G}(f)$ mainly stems from known component properties. In fact, because of practical considerations only the ceiling OFEs, i.e., the DUs, can be spatially distributed, while at the client EP, angular separation of OFE co-located in the same miniaturized MU devices is preferred. $\boldsymbol{Z}_0$ originates from distance-related path losses, emission patterns and collimated receiver opening angles, while multipath reflections are weak. Thus, $\boldsymbol{Z}_0$ is independent of the modulation frequency. This structure in the channel matrix allows efficient implementation and limits protocol overhead. In fact, while we saw that in radio communication over mobile multipath channels, adaptive subcarrier-dependent loading requires prohibitive amounts of signalling overhead, in OWC over LEDs, it is very feasible, and actually proven within the ITU G.9991 to be effective and efficient.

To evaluate the throughput of a DC-biased optical OFDM (DCO-OFDM) D-MIMO link, a singular value decomposition (SVD) of the overall channel matrix $\boldsymbol{H}(f)$ is computed and the overall throughput is estimated by (1):

$$R = \Delta_B \sum_{n=1}^{N} \sum_{k=1}^{K} \log_2 \left(1 + \frac{SNR}{N_T \eta_H \Gamma} \xi_k^2(f_n) \right) \tag{1}$$

where Δ_B is the bandwidth occupied by each subcarrier, N the number of subcarriers, K the rank of $\boldsymbol{H}(f)$, η_H the frequency-average path loss, $\Gamma = 10$ reflects typical system properties and, peak to average ratio (PAPR) DC biasing penalty [9, 26] and $\boldsymbol{\xi}_k(f_n)$ is the k-th singular value of $\boldsymbol{H}(f)$ at the n-th subcarrier. SNR is the signal-to-noise ratio referenced to the transmitter, thus defined as the transmit power P_T divided over the receiver noise spectral density N_0 times the total bandwidth $\Delta_B(f_N - f_1)$. The SNR can be influenced by spreading the power of the streams and over the frequency band in the most effective way within the power budget, but we assumed uniform power loading as done in ITU G.9991.

A simplified form is to use a single spatial stream with only one non-directional receiver photodiode (force $K = 1$), but to emit this from multiple ceiling locations. Then, the signal strength becomes the sum of multiple beams, with some phase delay effects if path length differs. In ELIoT, we evaluated and tested $K > 1$ in various ways. In the next sections, we initially address the combined challenge of how to build a D-MIMO system and a corresponding ceiling infrastructure and subsequently test to what extent the existing solution (in particular [25]) can already address this or need to be improved.

A. SDM and WDM-over-POF

POF can be attractive for the fronthaul of LiFi systems due to its do-it-yourself (DIY) ease of installation and its immunity against electromagnetic interference (EMI) [9]. To accommodate D-MIMO in the wireless link, two techniques can be used for POF-based LiFi fronthaul: space-division multiplexing (SDM) and wavelength-division multiplexing (WDM). SDM realizes point-to-point connections at the same wavelength over POF to connect each AP to the LiFi modem, as depicted in Figure 10(a). The main advantage of SDM is that there is no optical crosstalk in the optical feeding network. For the WDM approach, a single feeder POF is used to distribute the signals to the various APs by using different wavelengths, as illustrated in Figure 10(b). WDM can simplify the installation and maintenance, however it has higher complexity. With WDM, the amount of crosstalk between channels can be significant, if there is overlap in the optical spectrum. The crosstalk can be avoided using narrow optical light sources, such as laser diodes (LDs), however a lower cost system can be realized by using LEDs, which have a wider spectrum, thus higher spectral overlap. Yet, a new insight in ELIoT is that moderate colour crosstalk in the POF is not necessarily harmful as it can be mitigated by end-to-end MIMO (matrix inversion) processing that will be applied for the wireless link [9, 27].

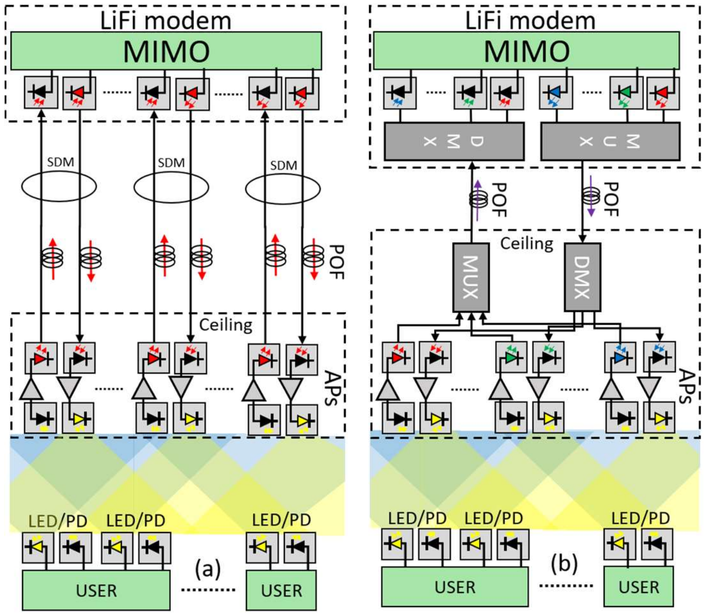

Figure 10: (a) SDM and (b) WDM approach using POF as the fronthaul of LiFi.

We measured SDM-over-POF with D-MIMO considering the channel response for the concatenation of POF and a wireless link. We only had access to commercially available red LEDs that would fit a POF connection, so we characterized the WDM-over-POF using LDs at 520 nm (green) and one at 658 nm (red). The WDM-over-POF link is characterized by measuring the losses due to light absorption in the POF and the crosstalk in the wavelength domain. We define crosstalk as the leakage between adjacent channels that can occur due to insufficient channel separation in the demultiplexer (DeMux). Our DeMux has a crosstalk level of -13dB and 3.2dB loss for the green and for the red channel a crosstalk level of -25.7dB and 3.6dB loss [28]. The losses for the green and red channel are asymmetrical due to differences in emitting and received optical power and due to different receiver sensitivities for either wavelength. Considering only the optical link for WDM, a throughput of 2.5 Gbps is achieved for the green wavelength channel and 4.3 Gbps for the red wavelength channel. To evaluate the performance of WDM-over-POF with D-MIMO, the POF link and the wireless link channel response are measured separately and then combined. The experimental setup is presented in Figure 11, where d1 is the distance between APS and user receiver, d2 is the distance between receivers and d3 is the distance between the APs. Two measurement scenarios are implemented to represent the downlink of a high bandwidth multi-user MIMO transmission for LiFi. In the first scenario, the access points and users located at d_1 = 100 cm, d_2 = 70 cm and d_3 = 70 cm. In the second scenario, the receivers are placed closer together, namely at d_1 = 50 cm, d_2 = 5 cm and d_3 = 35 cm.

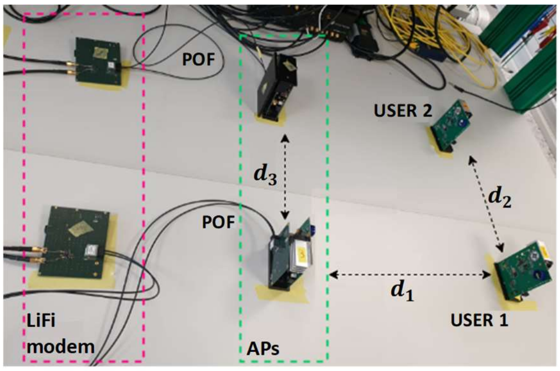

Figure 11: Experimental setup for LiFi D-MIMO using POF with SDM approach.

From the singular values of $\boldsymbol{H}(f)$, seen in Figure 12, and considering an SNR of 20 dB, the achievable throughput of the system is calculated using (1). Table 2 reveals that the performance for SDM is, as expected, better than for WDM, but only slightly so. In SDM, the absence of spectral overlap leads to a better conditioned matrix which increases the bit rate. Our WDM system further lacked margins to overcome unequal link budgets, which worsens after crosstalk removal due to noise enhancement in the MIMO equalizer. In particular, with available components, the green channel appeared challenging due to lower optical power and lower responsivity at the receiver. In both scenarios, the red channel can carry more data. We observed that the optical WDM link in isolation provides high performance, but end-to-end throughput reduces when the wireless channel is concatenated. The SDM have been done with LEDs rather than with lasers. Nonetheless, the end-to-end link is mostly limited by the wireless channel rather than by the POF [9].

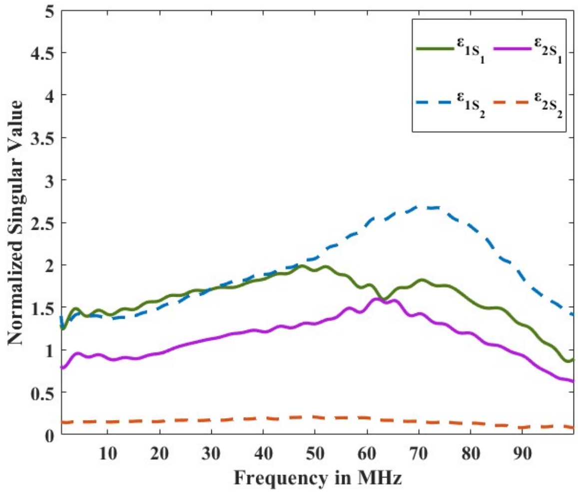

Figure 12: Normalized down-link singular values for SDM ,ξ_{1S1} and ξ_{2S1} for Scenario 1: spatially separated RX (solid lines) d_1= 100 cm, d_2= 70 cm, d_3= 70 cm, Scenario 2: (dashed lines) and ξ_{1S2} and ξ_{2S2} for Scenario 2: co-located RX:d_1 = 50 cm, d_2 = 5 cm, d_3 = 35 cm.

Table 2: Throughput evaluation of D-MIMO setup in two different scenarios.

D-MIMO SDM		D-MIMO WDM	
Scenario 1	586 Mbps	Scenario 1	484 Mbps
Scenario 2	421 Mbps	Scenario 2	369 Mbps

B. Passive all-optical OFE

To simplify the ceiling infrastructure for D-MIMO, it is attractive to avoid the need for electrical powering in the DUs (i.e., of the OFEs of the AP). One solution is to remotely feed optical fibres by a broadband LD and directly emit these signals from the fiber-end, without any optical-electrical-optical conversion [29]. In Figure 13(a,b) the system diagram for the downlink and uplink is presented, respectively. The transmitter is composed of a 1×2 power splitter and one distributed feedback (DFB) LD. The LD used emits red light at 658 nm, and is directly modulated in its linear region and then butt-coupled into the POF. The red LD emits an optical power of +2 dBm and it is biased at 80 mA. The light beam is transmitted through 5 m of POF, split and then transmitted through 1 m POF. In the DU where APs are placed, a lens is put in front of the POF-end to reduce the beam divergence. The standard polymethyl methacrylate (PMMA) POF has a numerical aperture of NA = 0.5 thus, if no lens is used, the light exiting the POF would be launched over an angular range of -30º to 30º. To create wireless cell of 45 cm, as shown in Figure 14, a lens is placed in a defocused position in the POF-end face. At the receiver side, the beam is received by another lens, coupled into a piece of POF and detected by an optical receiver composed of a silicon photodiode (PD) and a transimpedance amplifier (TIA). The PD+TIA has a detection bandwidth of 1.2 GHz.

The system schematic is presented in Figure 13, and the implementation in the laboratory is presented in Figure 14. The horizontal distance d_1 between the two POF-ends is set to 30 cm, while the vertical distance d2 between the POF outlets and receiver is set to 1.2 m. Measurements were performed by moving the receiver along the x axis, to simulate motion across cells. The x axis position 0 represents the middle between both POFs-end transmitters and the positions +15 and -15, represent the position in front of AP1 and AP2, respectively.

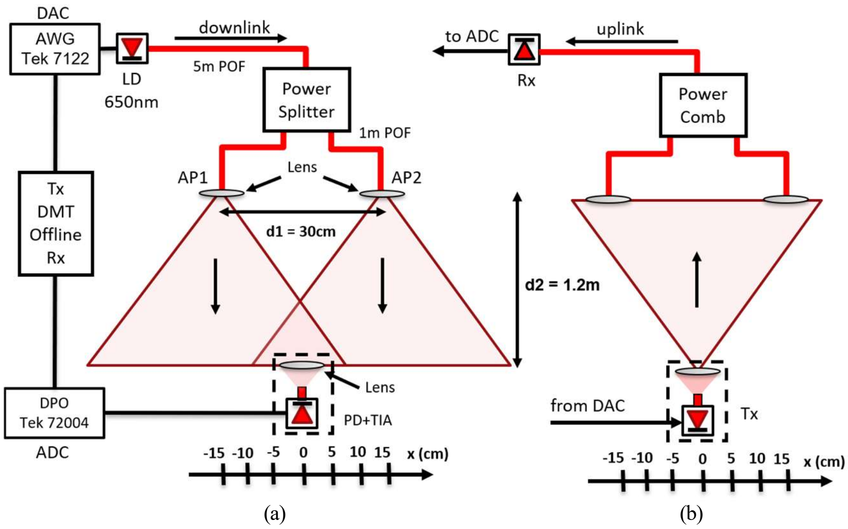

Figure 13: D-MIMO with Passive DUs: schematic, where the red path refers to (a) optical downlink, (b) uplink.

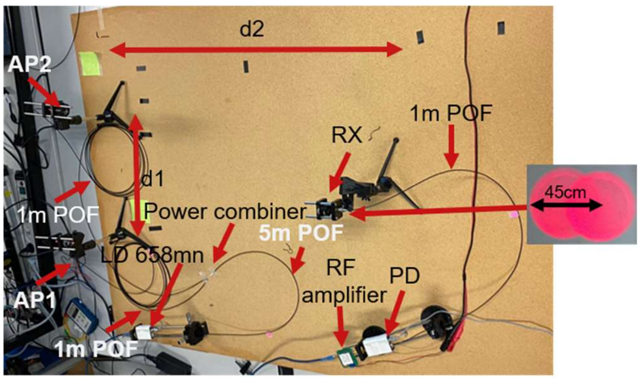

Figure 14: D-MIMO with Passive DUs: experimental setup.

To evaluate the achievable link performance considering user movement, transmissions using discrete multitone (DMT) modulation were realised. DMT, which is a (real-valued) baseband variant of OFDM, were used both for downlink and uplink. DMT was optimized by adaptive bit and power loading over 128 subcarriers, clipped at 9 dB, thus at $2\sqrt{2}$ times the rms signal strength. A bit error rate (BER) below the FEC level 1E-3 is achieved for all the presented results. An arbitrary waveform generator (AWG) works as a digital-to-analog converter (DAC) and generates the DMT signal. At the receiver, the signal is captured by a digital phosphor oscilloscope (DPO) that works as an analog-to-digital converter (ADC) sampling at 50 GSa/s. Offline signal processing is performed to obtain the throughput, SNR and BER counting for different positions of the user with respect to the POF outputs.

Figure 15(a) presents the throughput for various receiver positions for the downlink and uplink, respectively. The maximum throughput is obtained at the center, position 0, where the receiver is positioned in the middle of the overlapping area, achieving around 3.3 Gbps (downlink) and 2.6 Gbps (uplink) using DMT. At position 0, the receiver obtains signal contributions from both transmitters, which increases its SNR and, consequently, the throughput. When a user moves among cells, a throughput variation of 1.3 - 1.4 Gbps was measured. Figure 15(b) presents the performance of the POF output, measured directly at AP. Including wireless at x = 0, the received power is -13.5 dBm. Using Figure 15(b) for -13.5 dBm we can see a difference of 0.7 Gbps, and for x = -10, the difference becomes 1.2 Gbps. So, the user position with respect to APs has a considerable impact on the link performance.

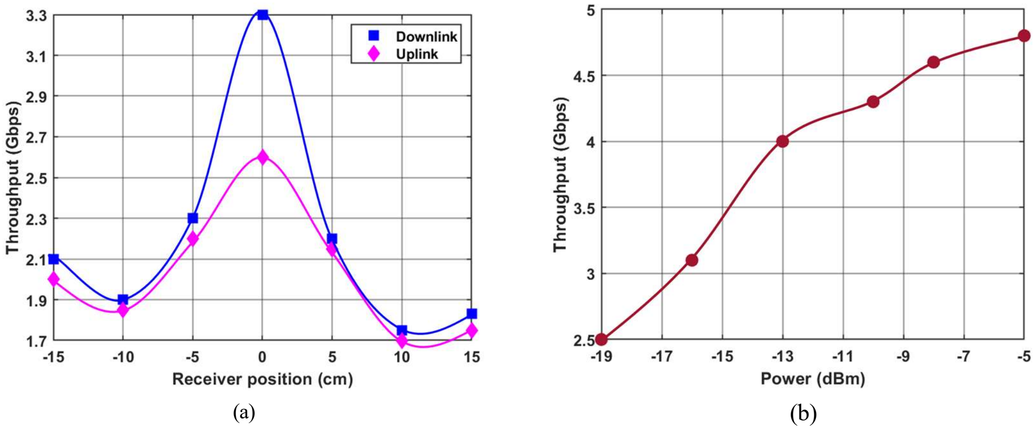

Figure 15: Link performance of DMT incl. 1.2m VLC transmission for the downlink and uplink (a) and POF throughput without wireless for various optical power (b).

VII. MEASUREMENTS OF MIMO PERFORMANCE WITH G.VLC AND G.HN PROFILES

The LiFi G.9991 standard [15] adopts many technical features which are important for high speed data transmission such as bit-loading, channel estimation from a previous standard (G.9960 to G.9964) also known as G.hn and includes some LiFi-specific features like handover. As these features were already defined in G.hn, these are present in G.hn chipsets. Chipsets and development kits with (sometimes minor) circuit deviations for each wired medium are readily available [25]. This accelerates LiFi developments and market introduction. Secondly, G.hn offers a robust and stable backbone for LiFi, with gigabit connections over any wire including powerline cables, coaxial cables, copper phonelines and POF. The powerline and phoneline profiles are able to run MIMO over a 100 MHz bandwidth and SISO over a 200 MHz bandwidth. The coax profile runs only in SISO mode up to 200 MHz bandwidth. Its PHY achieves a theoretical throughput of 2 Gbps over phoneline and coax, and of 1.5 Gbps over power lines. OFDM modulation uses a bandwidth of 50, 100 or 200 MHz with a maximum of 512 subcarriers. Each sub-carrier carries quadrature amplitude modulation (QAM) levels with up to 12 bits per symbol, according to an adaptive bit loading scheme. In contrast to radio standards designed for carrier-based transmission, G.hn works well over wired base-band channels, thus is well suited for LiFi channels. However, LEDs and large photodiodes are low-pass and may exhibit distortion due to non-linearity of the LED modules; additionally, LiFi applications, as any other wireless application, can have mobile users leading to time-varying channels. This poses the question whether G.vlc as it stands and as a derived technology from G.hn now solves all major LiFi problems.

A. Review of ITU based LiFi technology in the market

The availability of chipsets [25] allowed the commercial release of practical LiFi systems and built confidence in the standard. As examples, we can mention Signify's 2018 products offered a PHY rate up to 350 Mbps for downlink and 250 Mbps for uplink [30]. Meanwhile higher bit rates have also been tested. The AP combines the signals and sends the waveforms via analog wiring to up to six ceiling mounted OFE’s. Also, Fraunhofer HHI developed an advanced combiner prototype, based on POF which is more robust against electromagnetic interference in industrial scenarios also considered in ELIoT. OFEs generally comprise a LED driver (modulator), an IR-LED for the downlink transmitter and a photodiode with transimpedance amplifier for the uplink receiver. Fraunhofer HHI manufactures OFE prototypes with higher power and improved receiver sensitivity intended for larger coverage areas in industrial scenarios. Fraunhofer HHI released a USB LiFi prototype (LiFi NEON) to reach 1 Gbit/s in the downlink [31]. This is intended for dense user scenarios, e.g. in conference and classrooms. Moreover, there is an advanced outdoor LiFi prototype manufactured which allows 1 Gbit/s over 100 m for fixed wireless access scenarios investigated in ELIoT. These various products and prototypes show that early LiFi technology is flexible enough to cover a great variety of different use cases. Office use cases demand a moderate, but guaranteed throughput in a wide coverage area. According to feedback from the professional market, fairly uniform coverage with several meters range is considered more important than world-record throughput results in a tiny spot. Reliable, guaranteed low-latency QoS at some 100 Mbit/s/device satisfies the expected user experience. Gigabit performance is of interest in dense scenarios when aggregating the traffic of multiple users inside the coverage area. Up to 16 terminals can be served by the Signify LiFi AP in a managed TDMA scheme, within the coverage zone of six OFEs. OFDM allows reliable detection of signals from multiple OFEs. For the uplink direction an IR LED (940nm) is used that allows full duplex communication in the future. The optical power emitted in up- and downlink are well below the eye safety limit with a 40% margin. The Signify modem combines the signals and sends the waveforms via analog wiring to up to six ceiling mounted OFE’s. The diversity gain of the channel highly depends on the layout and the distances between all transmitters and orientation of receivers. Path loss can change quickly when the user moves around the room or rotates its device.

Meanwhile other vendors, e.g. OLEDCOMM, offer G.9991 LiFi solutions. In the ELIoT project, various experiments were conducted to verify the performance of G.9991 in different environments both for phoneline and powerline topologies. The results of these experiments are shared in this section.

B. Measured performance under static conditions

The experimental setup consists of a 2x2 MIMO LiFi system as shown Figure 16: On one side of the system, there is a ceiling node representing a LiFi access point and on the other side a user node. Both user and ceiling nodes have a Maxlinear G.hn MIMO evaluation kit connected to two Trulifi optical frontends from Signify [32]. Each Trulifi transceiver has one IR-LED and one PD for bidirectional optical/electrical and electrical/optical conversion. The transceivers are connected to the evaluation kit PCBs with CAT5 cables. Connected to each evaluation kit PCB, there is one laptop running iPerf software to measure the network throughput while operating under G.hn MIMO profile.

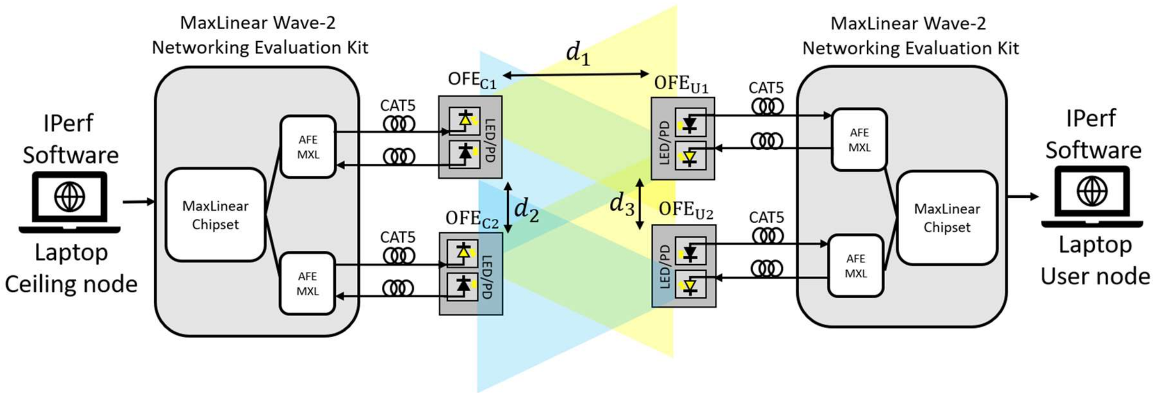

Figure 16: Test setup for G.vlc MIMO LiFi with phoneline or powerline profiles.

C. G.hn Coax Mode: SISO with Multiple Emitters (rank $K = 1$)

In Coax mode, no MIMO features are available. That does not preclude the creation of diversity channel, even if we only use one photo diode in the AP ($N_R = 1$). This mimics MISO, but without the ability to apply a transmitter phase compensation. Having calibrated our SISO model in [18], we now rely on such model: using L OFE's in the ceiling, having a pathloss h_{l1}, for the l-th OFE TX to the common 1st receiver, the rate expression (1) for a distortion-free LED reduces to

$$R = \Delta_B \sum_{n=1}^{N} \left\lfloor \log_2 \left(1 + \frac{P_T}{N_T \eta_H \Gamma N_0} \left[\sum_{l=1}^{L} h_{l1} \exp\left\{ -2\pi j \frac{d_l}{c} f_n \right\} \right]^2 \right) \right\rfloor \quad (2)$$

Here, we modelled unequal cable lengths d_l causing an extra latency, dependent on the propagation speed c in the cable or POF. In fact, MIMO channel estimation could facilitate a frequency-dependent phase correction for d_l, but the Coax mode does not support that. The use of an integer (or even) number of bits per QAM constellation is reflected in the rounding brackets ⌊ ⌋.

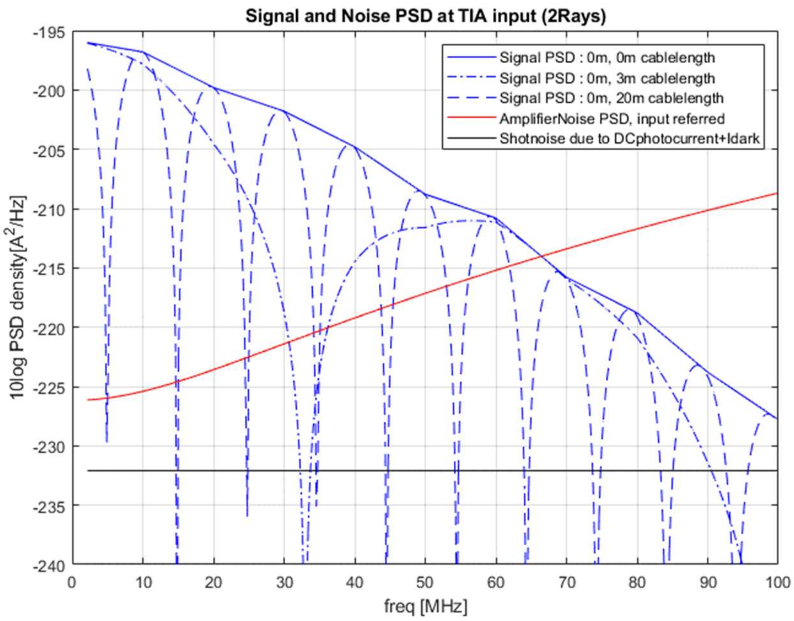

a)

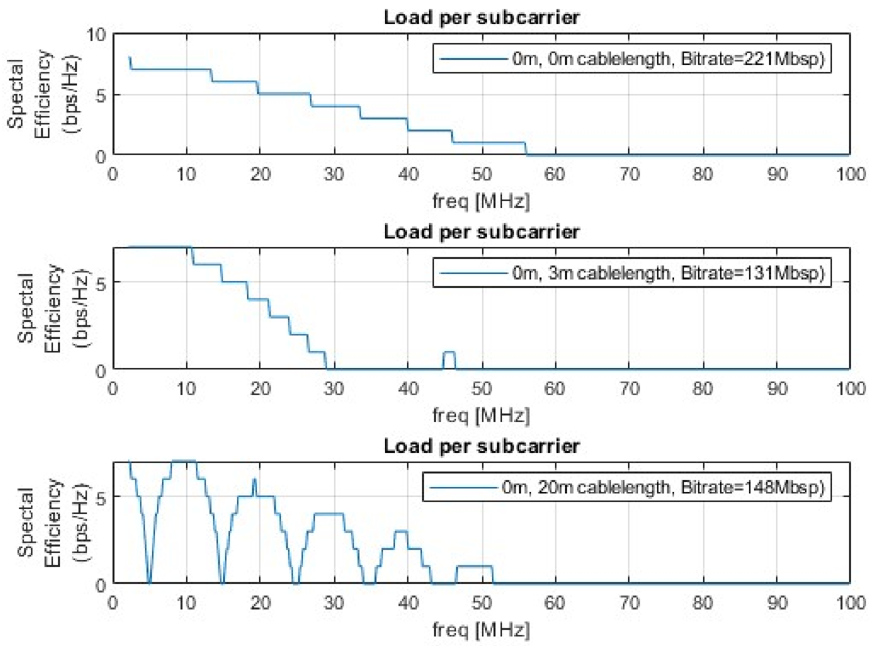

b)

Figure 17: (a) Received signal strength and noise floor for a two-ray SISO transmission in the middle of two emitters connected with a cable length difference of 0, 3 and 20 meters. (b) resulting estimated bit loading.

Figure 17 shows a frequency response for one OFE-OFE link measured with a spectrum analyser for a typical OFE implementation, extended to a two-ray path originating from the sample signal travelling via two parallel cables. The TIA and detector produce non-white noise as also plotted in Figure 17. Theoretical throughputs are somewhat larger than measured throughput, firstly because of different Signal Power to Noise ratios and secondly because we have neglected distortion here. We conclude that the adaptive bit loading can track the channel and its combined interference pattern. Small differences in cabling reduces the throughput significantly, from 221 Mbit/s for equal cable lengths to 131 Mbit/s for a 2 meter difference which creates one notch around 33 MHz. At very long distances, the channel response exhibits many notches and the throughput converges to 148 Mbit/s, surprisingly a bit higher than for smaller cable length differences. This throughput at unequal feeder lengths still are better than what would be achieved without adaptive bit loading, just by error correction coding across the notches. The latter coding solution is for instance used in single-frequency networks for digital audio broadcasting (DAB) where user-specific bit-loading is not possible. Our bit loading, is plotted in Figure 17b.

D. G.hn Phone line mode

In the first experiment, we investigate the performance of a 2x2 MIMO LiFi system using G.hn MIMO 100 MHz phoneline profile. Four different scenarios are considered and the measured throughput for each of them is shown in Table 3: In Scenario 1, the OFEs are 1 m apart from each other, i.e., $d_1 = d_2 = d_3 = 1$ m. In this case, the crosstalk channels have low gain, and spatial multiplexing performs well. The system achieves ~500 Mbps for both downlink and uplink. In the second scenario, we placed the luminaires at the user side very close to each other, i.e., d_3~2 cm, just separated by a small angle. The user node was then placed in the middle of the coverage area of the ceiling node OFEs at a distance of 1 m. Now, the channel matrix becomes close to singular and the downlink throughput drops by more than one half and the uplink throughput decreased even more. We conclude that the system does not adapt well to handle crosstalk and does not switch to a diversity mode in a highly correlated channel. In the third scenario, we kept the OFEs of the user side as in Scenario 2 but, we placed the user in front of OFE_{C2}. In this case, crosstalk is very high, so a change from MIMO spatial multiplexing to spatial diversity would be required. Unfortunately, the current version of the chipset, anticipating a fixed phoneline, was not programmed to switch its transmission mode. Lacking such adaptation, the measured performance was very low. In a fourth scenario, a piece of cardboard is placed in front of OFE_{U1} to mimic a link blockage. Although one of the MIMO links is unblocked and still available for communication, the phoneline profile did not adapt well and the throughput fully collapsed.

Table 3: Measured throughput of G.hn MIMO 100 MHz with phoneline profile

Scenario	Downlink [Mb/s]	Uplink [Mb/s]
1	511	501
2	200	59.9
3	18.5	42.3
4	0.91	3.14

E. G.hn Powerline profile

In the second experiment, we used the G.hn MIMO 100 MHz powerline profile. In Scenario 5, we have again a low correlated MIMO LiFi channel, i.e. $d_1 = d_2 = d_3 = 1m$. In this case, spatial multiplexing performs well, but the achieved throughput is almost half of the achieved throughput with the phoneline profile for a similar setting. This is due to the additional overhead for more robust coding and to address PLC EMI for instance with spectral notches in the powerline profile. In Scenario 6, OFE_{C1} is blocked with a piece of cardboard. In contrast to the performance of phoneline profile in Scenario 4, the powerline mode is able to establish communication over the unblocked link and achieve a throughput of 108 Mbps in the downlink channel, which is approximately half of the performance in Scenario 5. In Scenario 7, the OFEs at the user side are placed close to each other and placed in the middle of the coverage area - similar to Scenario 2. Although this represents a highly correlated channel, the measured throughput of 115 Mbps for the downlink and 112 Mbps for the uplink are much better than the phoneline case. In Scenario 8, the user node is placed in front of OFE_{C2}, and a piece of cardboard was placed in front of OFE_{C1} . The measured throughput was 108 Mb/s for the downlink and 101 Mbps for the uplink. In Scenario 9, OFE_{C2} was unblocked and the measured throughput increases to 131 Mbps in the downlink channel and 133 Mbps in the uplink channel. For both up and down link directions, the MIMO options show 12% – 30% more throughput than the MISO arrangements.

Table 4: Measured throughput of G.hn MIMO 100 MHz for powerline profile

Scenario	Downlink [Mb/s]	Uplink [Mb/s]
5	191	Not measured
6	108	Not measured
7	115	112
8	108	101
9	131	133

F. Measured performance under dynamic conditions

Tests showed that some blockage is addressed as the system adapts from MIMO to MISO mode of operation. However, we also recorded instances in which the throughput collapsed after blockage and did not recover for minutes. The latter demonstrates the need for further improvement in the chipset (hardware/firmware) and the signalling to track changes in channel characteristics rapidly enough.

Figure 18 reports an experiment with Scenario 7, achieving 138 Mb/s. At 104 s, the user-side OFEs were placed in front of OFE_{C2} (highly correlated channels) and the throughput reduced to 133 Mb/s. Thereafter, OFE_{C1} was blocked at 205 s, further reducing the throughput to 102 Mb/s. When the blockage was removed at around 287 s, the throughput recovered to 130 Mb/s. At 407 s, OFE_{C2} was blocked that resulted in collapse of communication for the following 60 seconds after which the throughput started to toggle between 20 Mb/s and 50 Mb/s. When the blockage was removed at 611 s, the 130 Mb/s throughput was regained.

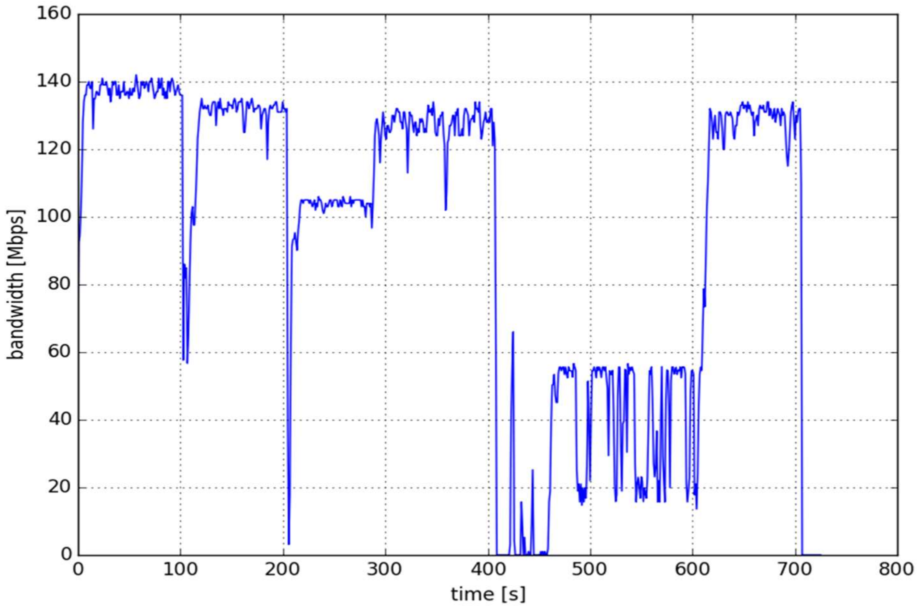

Figure 18: Link performance when moving user-side OFEs, blocking and un-blocking one of the ceiling -side OFEs.

In summary, although the phoneline profile gives higher throughputs under static well-conditioned spatial multiplexing modes, current implementations do not cope well with channel changes. The powerline profile, despite its lower overall throughput, can handle some dynamism in the communication channel. However, since the PLC modem is developed/optimized for a powerline medium, it lacks features to handle fast changes in channel characteristics arising from mobile users in LiFi. Evidently, a new optimized mode for lighting communication is desirable.

VIII. Roadmap for Implementation

ITU-T approved the ITU-T G.9991 Recommendation for LiFi in 2020. The DCO-OFDM variant of this Recommendation is the base of most developments in the ELIoT project. The goal of this recommendation is to provide a fast-to-market LiFi system with adequate performance to cover the main industrial, enterprise and residential use cases. By reusing the OFDM engine with its adaptive bit loading, already successfully used in other Recommendations (i.e., in the ITU-T G.hn family, aimed to cover in-home connectivity over coaxial, phone and power lines), the resulting ITU-T G.9991 document enables LiFi systems by reusing existing chipsets. This way, early LiFi products can benefit from high-volume, low-cost integrated solutions while providing a good adaptation to the specifics of the majority of LiFi use cases. This approach allows integrators to rapidly create an early mass market for LiFi systems with a reasonable investment.

In parallel, the ITU-T Q18/15 group within ITU-T is evolving the Recommendation to cover remaining scenarios and new scenarios and requirements identified during the first LiFi deployments in industry and further scenarios identified within the ELIoT project that were not contemplated in the first version of the Recommendation. Inter-domain handover and interference management is one example that has been added to the G.9991 framework through an amendment to the standard. The work continues to add new features in the standard that will lead in the future to new amendments or a new revision of the Recommendation. This will allow a new generation of LiFi chipsets that will incorporate specific LiFi hardware macros allowing new applications (e.g., positioning). New evolutions are also expected to address power reduction and better integration with other technologies to foster the adoption of LiFi technology in mobile devices. In this sense, new features have been identified within ELIOT project. Some of them can be incorporated into the current standard and in current generation chipsets through software development while others will necessitate a change of hardware and will take some time to be available since LiFi must first generate a market that is wide enough to justify a new silicon investment or to continue the strategy of piggybacking on existing implementations. Among the new required features identified by ELIOT project, we may mention faster channel estimations for enhanced mobility support, profile selection to adapt the characteristics of the transmission to the channel specifics and, last but not least, the inclusion of MIMO technologies, currently not in the standard and with a limited support in the existing hardware. An evolution of MIMO techniques for LiFi as the ones investigated in the project (multi-user environments) would represent an important step in the performances achieved by LiFi systems.

Finally, we mention an integration opportunity of LED front end functionality with the existing general purpose analog front ends used so far, for instance for PLC, Coax or phone lines.

As a summary, we can say that the approach used so far allows LiFi vendors to leverage a broad portfolio of existing ITU-T G.hn compliant chipsets in their early products and facilitate interoperability of early solutions early on, reusing existing ecosystems and lower the barriers to deploy this new technology. This approach shall be gradually transformed in more specialized LiFi solutions as the market grows and higher volumes become possible.

IX. Indoor Positioning

Besides communication, smart manufacturing calls for positioning to facilitate various new Industry 4.0 applications. For example, reliable indoor positioning is necessary for using intelligent transport systems (ITS) that transport parts on pallets from predefined locations to other predefined locations. It is usual that transport systems in factories and warehouses travel along predefined paths, defined by inductive loops or optical markers on the floor. But these systems are not flexible, and modifications need effort. LiFi enables localization beyond predefined paths and allows extended positioning use cases due to more degrees of freedom. For example, a transport system can determine a new path on-demand to drive around an obstacle that occurred on the planned path. In addition, there are new opportunities when production resources can be located on-demand. For example, its position can be displayed on a digital factory map. This makes it possible to find a tool, a container with raw material or (semi-) finished products needed in a few seconds, which supports the work of machine operators and production planners. In addition, real-time positioning of mobile devices can support technical maintenance staff or production managers. For example, tablets can support them by using the position information to display position-based information such as dashboards with machine data of the nearest machine(s).

In the ELIoT project, we propose to realize positioning based on a multi-lateration algorithm, which measures the wireless propagation times between a mobile device and multiple LiFi APs at the ceiling [25, 33]. The ranging or timing advance algorithms for positioning are well understood and used in fixed and mobile access systems [18]. The accuracy of the result depends primarily on the quality of estimating the time-of-flight. To address the inherent synchronization challenges between mobile and ceiling units, an active ping-pong protocol is used to measure the round-trip time. This allows, in combination with standard techniques for clock offset estimation, an accurate estimation of the time-of-flight. The overall principle of LiFi based positioning is shown in Figure 19 [17]. Figure 19a) shows the ranging by multiple transmitter units, Figure 19b) the signal structure based on the G.hn standard and Figure 19c) the ping-pong protocol for the estimation the round-trip time. To confirm this concept, a series of simulations and measurements have been carried out in ELIoT. First results [17] showed the feasibility of the concept by simulations in a 3D environment as well as by ranging experiments of LiFi point-to-point links. Further investigation addressing 3D positioning Scenario are presented in this section. The setup is show in Figure 20 and consists of 4 Tx units at fixed positions a single Rx units. The signal progressing, as shown in Figure 19 is performed in MATLAB and the signal conversion by DACs and ADCs. For the measurements, the Rx units were at multiple positions and the performance at each of them evaluated.

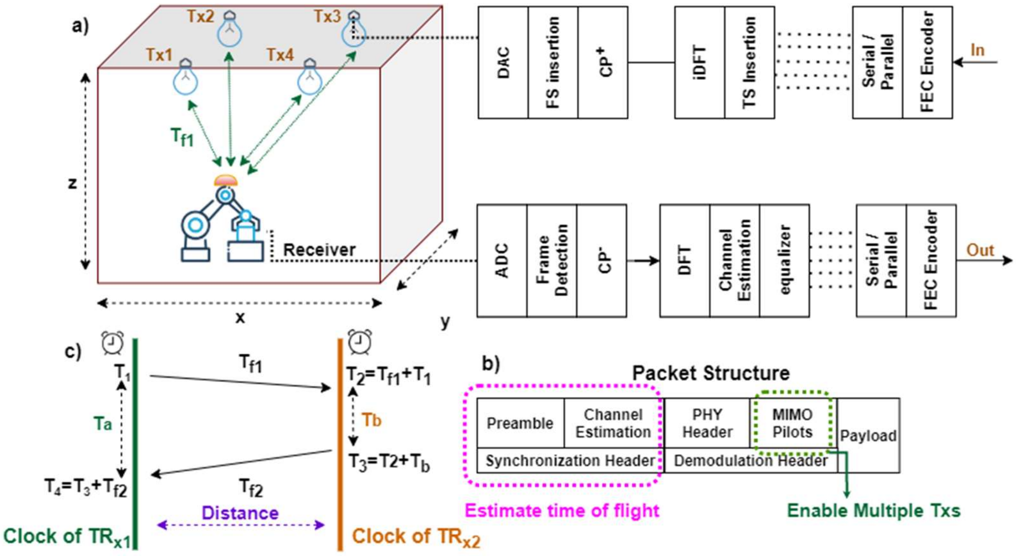

Figure 19: a+c) Principle of LiFi based positioning, b) signal structure

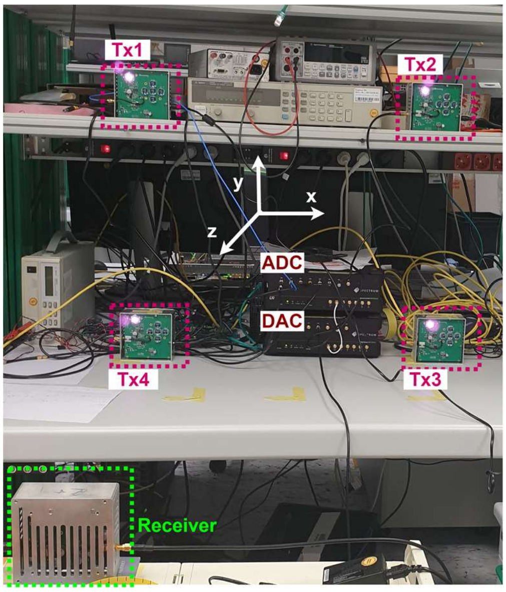

Figure 20: Measurement setup for 3D evaluation,

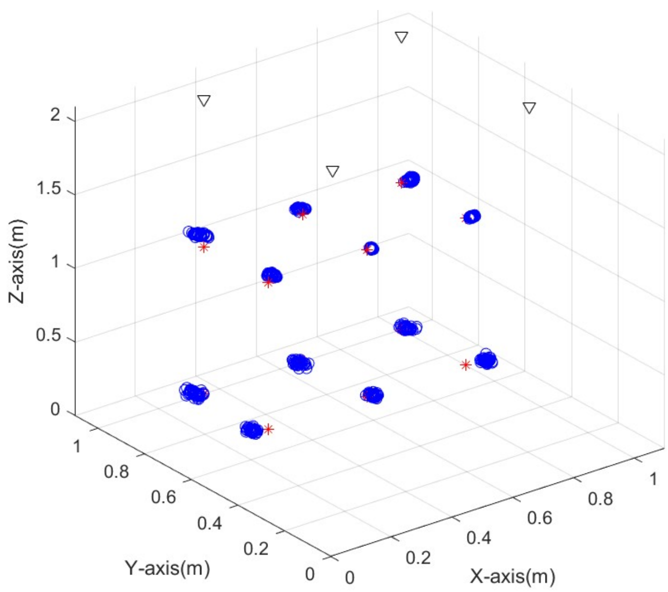

Figure 21: Estimated (denoted by blue circles) versus real position (denoted by red stars) for multiple receiver positions. Transmitter positions are denoted by black triangles.

Figure 21 shows the estimated (blue circle) versus the actual positions of the receiver for 40 measurements (iterations) at each of the 12 positions. The transmitter positions are indicated by the black triangles. The difference between estimated and real receiver positions are overall very small, with higher deviation towards the edges of room. Figure 22(a) shows the resulting average mean-square errors (MSE), for each the x- ,y- and z-axis and for each Rx location taking 40 independent measurements into account. The x-axis shows a generally higher MSEs and the errors of the z-axis are the smallest, with one exception. The smaller error for the z-axis can be attributed to the alignment of the setup. In Figure 22(b) the combined x,y,z error is shown for three Rx positions over 40 measurements. There are two observations: First, there is a different offset error for each position, with Rx(1,0.72,0) the highest and Rx(0.67,0.725,0) the lowest. The offset error can be attributed to non-ideal calibration, which was only performed in 1D for one location only. Note that the offset error is smaller in the centre position between the four transmitters (blue curve) and is higher at the edges (red curve). Second, there is a second type of error caused by the signal noise. This random error is indicated by the variation around the offset error and is magnitude is directly related to the SNR and to the distance between Tx and Rx. The offset error can be minimized by a more careful initial calibration of the system before the actual measurements and the second error by applying a stronger averaging, i.e. taking more measurements for each position into account.

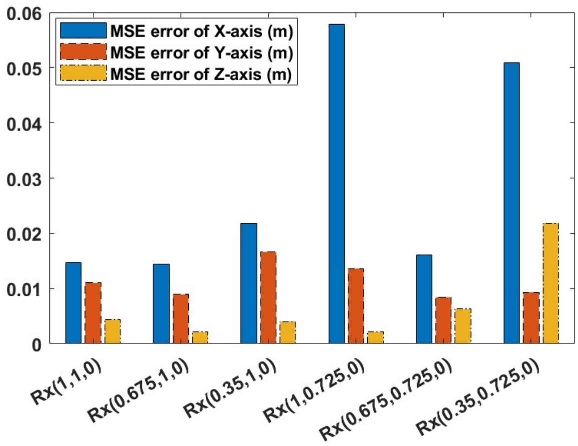

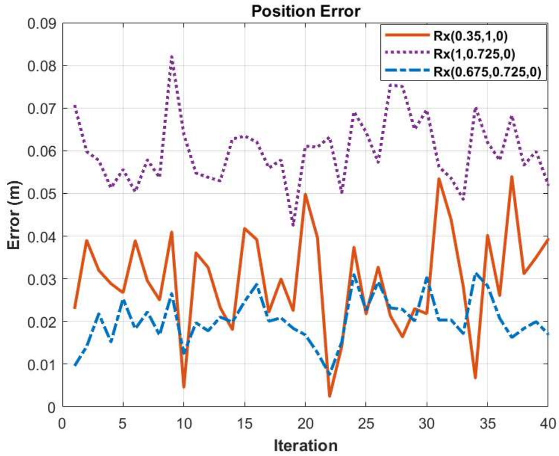

Figure 22: Mean square error (MSE) of x,y,z for selected Rx position (a) and combined error or three receiver positions over 40 measurements (b).

A. Possible Roadmap for adding positioning to G.vlc

Enabling real-time positioning requires integration into a LiFi chipset. Today's chipsets only partly support the proposed concept. The ELIoT project is working with a chipset from MaxLinear that implements the ITU-T G.9991 recommendation [25]. With this chipset a coarse round-trip time estimation can already be achieved by using the time tagging capabilities. More precise timing information can be extracted from the channel frequency response (CFR) as demonstrated by the ELIoT experiments. For a next generation chipset, new APIs have to be developed in the PHY to provide information on the SNR and CFR to the higher layers.

The high-level architecture of the a digital baseband G.9991 chipset is shown in [25] (page 9). The baseband chip decodes the frames coming from the channel and injects frames in the channel through an analogue frontend chip that performs the signal adaptation to the medium. The positioning techniques explained in [18] can run application programming interfaces (API). The techniques that have been described in [18] can already be partially implemented using commercially available chipsets. The chipset can make use of some of the functionalities and framing of the standard that allow refining the procedure explained in [25].

X. SUMMARY

The ELIoT project addresses LiFi features that enable the next generation of IoT applications for various indoor and outdoor use cases in the industry, office, commercial and consumer sectors. We presented a distributed MIMO wireless topology which can be supported by SDM/WDM fronthaul transport of waveforms via a plastic optical fibre. Besides these, we described security aspects and various concepts for seamless handovers between the light-based access points and also to a radio-based infrastructure such as a 5G network. We have shown that the LiFi technology has the potential to provide both precise indoor localization and high-speed data transfer. The results presented indicate that the PHY offers indoor positioning, with an average accuracy of 5 cm, what even the most modern radio-based systems cannot achieve. D-MIMO light communication enhances reliability and delivers throughputs of hundreds of megabits per second. Concepts to further increase the performance of LiFi systems have already been identified. These features are currently being tested towards use-case demonstrations. We foresee that LiFi systems can complement upcoming 6G systems by offering high QoS link in hotspots.

XI. FUNDING

We gratefully appreciate the European Commission for financially supporting the H2020 Innovation Action project "ELIoT" through grant 825651.

XII. COMPETING INTERESTS

The ELIOT consortium consists of industrial partners who have an interest in a broad adoption and commercial success of LiFi and its application via standardized and interoperable solutions, and a number of independent academic partners.

XIII. AUTHOR CONTRIBUTIONS

All authors have contributed toward this work as well as in compilation of this manuscript. The authors read and approved the final manuscript.

References

[1] Jing et al., “The Road Towards 6G: A Comprehensive Survey,” *IEEE Open Journal of the Communication Society,* vol. 2, pp. 334-336, 2021.

[2] S. Panwar, “Breaking the Milisecond Latency Barrier,” Oct 2020. [Online]. Available: https://spectrum.ieee.org/breaking-the-latency-barrier. [Accessed August 2021].

[3] Müller et al., “Leverage LiFi in Smart Manufacturing,” in *2020 IEEE Globecom Workshops (GC Wkshps)*, Taipei, Taiwan, 2020.

[4] J. P. Linnartz et al., “ELIoT: New Features in LiFi for Next-Generation IoT,” in *2021 Joint European Conference on Networks and Communications & 6G Summit (EuCNC/6G Summit)*, 2021.

[5] Bober et al., “A Flexible System Concept for LiFi in the Internet of Things,” in *ICTON*, 2020.

[6] T. Fath and H. Haas, “Performance Comparison of MIMO Techniques for Optical Wireless Communications in Indoor Environments,” *IEEE Transactions on Communications,* vol. 61, no. 2, pp. 733-742, February 2013.

[7] L. Zeng et al., “High data rate multiple input multiple output (MIMO) optical wireless communications using white led lighting,” *IEEE Journal on Selected Areas in Communications,* vol. 27, no. 9, pp. 1654-1662, December 2009.

[8] P. Wilke Berenguer et al, “Optical Wireless MIMO Experiments in an Industrial Environment,” *IEEE Journal on Selected Areas in Communications,* vol. 36, no. 1, pp. 185-193, January 2018.

[9] S. M. Kouhini et al., “Distributed MIMO Experiment Using LiFi Over Plastic Optical Fiber,” in *2020 IEEE Globecom Workshops (GC Wkshps)*, Taipei, Taiwan, 2020.

[10] C. van den Broek and J.P. M. G. Linnartz, , “A simulation study of space and time reservation multiple access,” in *6th International Symposium on Personal, Indoor and Mobile Radio Communications*, 1995.

[11] K. L. Bober et al., “Distributed Multiuser MIMO for LiFi in Industrial Wireless Applications,” *Journal of Lightwave Technology,* vol. 39, no. 11, pp. 3420-3433, 1 June 2021.

[12] A. Maeder et al., “Towards a flexible functional split for cloud-RAN networks,” in *2014 European Conference on Networks and Communications (EuCNC)*, 2014.

[13] T. Metin, M. Emmelmann, M. Corici, V. Jungnickel, C. Kottke and M. Müller, “Integration of Optical Wireless Communication with 5G Systems,” in *2020 IEEE Globecom Workshops (GC Wkshps, 2020)*, Taipei, Taiwan, 2020.

[14] T.E.B. Cunha, W.X. Fan, X. Deng, J. -P.M.G. Linnartz, “A Space-frequency Power Allocation Algorithm for MIMO OWC Systems over Low-Pass Channels,” in *2020 1st Optical Wireless Communication Conference* , 2020.

[15] International Telecommunication Union Recommendation G.9991-202104 Amd.2, “High-speed indoor visible light communication transceiver – System architecture, physical layer and data link layer specification,” 2021.

[16] M. Hinrichs et al., “A Physical Layer for Low Power Optical Wireless Communications,” *IEEE Transactions on Green Communications and Networking,* vol. 5, pp. 4-17, March 2021.

[17] J. Beysens, J. -P. M. G. Linnartz, D. Van Wageningen and S. Pollin, “TDMA Scheduling in Spatially Extended LiFi Networks,” *IEEE Open Journal of the Communications Society,* vol. 1, pp. 1524-1538, 2020.

[18] S. M. Kouhini et al., “LiFi Positioning for Industry 4.0,” *IEEE Journal of Selected Topics in Quantum Electronics,* vol. 27, pp. 1-15, Nov-Dec 2021.

[19] J. -P. M. G. Linnartz, X. Deng and P. Van Voorthuisen, *Impact of Dynamic LED Non-linearity on DCO-OFDM Optical Wireless Communication,* August 2021.

[20] IEEE, “IEEE Standard for Local and metropolitan area networks--Port-Based Network Access Control,” [Online]. Available: https://standards.ieee.org/standard/802_1X-2010.html.

[21] IETF, “Internet X.509 Public Key Infrastructure Certificate and Certificate Revocation List (CRL) Profile,” [Online]. Available: https://tools.ietf.org/html/rfc5280.

[22] IETF, “Remote Authentication Dial In User Service (RADIUS),” [Online]. Available: https://tools.ietf.org/html/rfc2865.

[23] IETF, “Extensible Authentication Protocol (EAP),” [Online]. Available: https://tools.ietf.org/html/rfc3748.

[24] IEEE, “IEEE Standard for Information technology--Telecommunications and information exchange between systems Local and metropolitan area networks--Specific requirements - Part 11: Wireless LAN Medium Access Control (MAC) and Physical Layer (PHY) Specifications,” [Online]. Available: https://standards.ieee.org/standard/802_11-2016.html.

[25] Maxlinear, “88LX5152, 88LX5153 Wave-2 G.hn Digital Baseband (DBB) Processor,” 2020. [Online]. Available: https://https://www.maxlinear.com/ds/88lx515288lx5153:pdf.

[26] T. E. Bitencourt Cunha, J. M. G. Linnartz and X. Deng, “Throughput of Optical WDM with Wide LED Spectra and Imperfect Color-detecting Filters,” in *2020 29th Wireless and Optical Communications Conference (WOCC)*, 2020.

[27] Wu et al., “Hybrid LiFi and WiFi Networks: A Survey,” *IEEE Communicatinos Surveys & Tutorials,* vol. 23, no. 2, pp. 1398-1420, 2021.

[28] C.R.B. Corrêa et al., “WDM over POF for D-MIMO LiFi system,” in *1st Optical Wireless Communication Conference - Online*, 2020.

[29] C. R. B. Corrêa, F. M. Huijskens, E. Tangdiongga and A. M. J. Koonen, “Luminaire-Free Gigabits per second LiFi Transmission employing WDM-over-POF,” in *2020 European Conference on Optical Communications (ECOC)*, 2020.

[30] A.M. Khalid et al., "Productization Experiences of G.vlc (ITU) based LiFi System for high Speed Indoor Wireless Access," in *1st Optical Wireless Communication Conference (OWCC 2020)*, 2020.

[31] LiFi Neon, [Online]. Available: https://lifi-neon.de. [Accessed September 2021].

[32] Signify Trulifi, [Online]. Available: https://www.assets.signify.com/is/content/PhilipsLighting/Assets/signify/global/20200416-specsheet-trulifi-6002.pdf.. [Accessed 15 April 2021].

[33] S. Mardanikorani, X. Deng, J. -P. M. G. Linnartz and A. Khalid, "Compensating Dynamic Nonlinearities in LED Photon Emission to Enhance Optical Wireless Communication," *IEEE Transactions on Vehicular Technology,* vol. 70, no. 2, pp. 1317-1331, 2021.

Abbreviations

Internet of Things	IoT	Radio Access Network	RAN
Multiple Input Multiple Output	MIMO	Time Division	TDMA
Local Area Network	LAN	Modulation-Frequency Division	FDMA
Quality of Service	QoS	Code Division	CDMA
Enhance Lighting for the Internet of Things	ELIoT	Wavelength Division	WDMA
Plastic Optical Fiber	POF	Carrier Sense Multiple Access – Collision Avoidance	CSMA/CA
Physical Layer	PHY	End Points	EP
Medium Access	MAC	Common Channel	CC
Direct Current	DC	Lifi Controller	LC
Orthogonal Frequency Division Multiplexing	OFDM	Precision Time Protocol	PTP
Line of Sight	LoS	Singular Value Decomposition	SVD
Pulse Amplitude Modulation	PAM	Do-It-Yourself	DIY
Visible Light Communication	VLC	Electromagnetic Interference	EMI
Spatial Time Division Multiple Access	Spatial TDMA	Space-Division Multiplexing	SDM
Access Point	AP	Wavelength-Division Multiplexing	WDM
Central Unit	CU	Laser Diode	LD
Base Band	BB	Polymethyl Methacrylate	PMMA
Distributed Units	DUs	Transimpedance Amplifier	TIA
Optical Front Ends	OFEs	Discrete Multitone	DMT
Mobile Unit	MU	Bit Error Rate	BER
Power Line Communication	PLC	Arbitrary Waveform Generator	AWG
Signal-to-noise ratio	SNR	Digital-To-Analog Converter	DAC
Modulation and Coding Scheme	MCS	Analog-To-Digital Converter	ADC
User Equipment	UE	Quadrature Amplitude Modulation	QAM
Core Network	CN	Digital Audio Broadcasting	DAB
Internet Key Exchange	IKE	Intelligent Transport Systems	ITS
Extensible Authentication Protocols Authorization and Key Agreement	EAP-AKA	Average Mean-Square Errors	MSE
Pairwise Master Key	PMK	Channel Frequency Response	CFR
Carrier-sense Multiple Access	CSMA	Application Programming Interfaces	API
Software Defined Networking	SDN	Time Division	TDMA